Available online at www.sciencedirect.com
SCIENCE DIRECT®
C. R. Physique 6 (2005) 836–847
COMPTES RENDUS PHYSIQUE
http://france.elsevier.com/direct/COMREN/

Spectroscopy and planetary atmospheres/Spectroscopie et atmosphères planétaires

Ultraviolet and visible spectroscopy and spaceborne remote sensing of the Earth's atmosphere

Kelly Chance

Harvard-Smithsonian Center for Astrophysics, Atomic and Molecular Physics Division, 60 Garden Street, Cambridge MA 02138, USA

Available online 3 October 2005

Abstract

Current capabilities for ultraviolet and visible spectroscopic measurements of the Earth's stratosphere and troposphere are reviewed. Atmospheric spectral properties are described. The major measurement geometries and types are presented. Instrumental, spectroscopic, and radiative transfer modeling challenges are discussed. Current and planned satellite instruments for this field, with their measurement properties, spectral coverage, and target molecules are presented. Measurement examples include stratospheric and tropospheric NO_2, tropospheric BrO in the polar spring, global tropospheric HCHO, and tropospheric ozone measurements from the nadir geometry. The field is shown to be sufficiently mature that global measurements of atmospheric pollution from space may be undertaken. ***To cite this article: K. Chance, C. R. Physique 6 (2005).***
Published by Elsevier SAS on behalf of Académie des sciences.

Résumé

Spectroscopie dans l'ultraviolet et le visible et télédétection spatiale de l'atmosphère terrestre. Les possibilités actuelles de mesure spectroscopique de la stratosphère et de la troposphère terrestres sont passées en revue avec les caractéristiques spectrales de l'atmosphère. Nous présentons également les principaux types et géométries de mesure et discutons les défis, qu'ils soient instrumentaux, spectroscopiques, ou concernant les modèles de transfert radiatif. Sont également présentés dans cet article les instruments satellitaires actuels et prévus, en détaillant leurs caractéristiques instrumentales, leurs couvertures spectrales et les molécules qui sont leurs cibles. Nous donnons des exemples d'observations au nadir dans les cas du NO_2 stratosphérique et troposphérique, du BrO troposphérique au printemps polaire, du HCHO troposphérique total, et de l'ozone troposphérique. Nous montrons que le domaine est aujourd'hui suffisamment mur pour que des mesures globales de la pollution atmosphériques à partir de l'espace soit possibles. ***Pour citer cet article : K. Chance, C. R. Physique 6 (2005).***
Published by Elsevier SAS on behalf of Académie des sciences.

Keywords: Ultraviolet spectroscopy; Visible spectroscopy; Atmospheric remote sensing; Stratospheric composition; Tropospheric composition; Radiative transfer modeling; Chemistry and transport modeling

Mots-clés : Spectroscopie ultraviolet ; Spectroscopie visible ; Télédétection atmosphérique ; Composition de la stratosphère ; Composition de la troposphère ; Transfert radiatif ; Modélisation du transport et de la chimie

E-mail address: kchance@cfa.harvard.edu (K. Chance).

1631-0705/$ – see front matter Published by Elsevier SAS on behalf of Académie des sciences.
doi:10.1016/j.crhy.2005.07.010

1. Introduction

This article provides an overview of current results and capabilities which show how ultraviolet and visible spectroscopy is used to elucidate important properties about the Earth's stratosphere and troposphere. This is now a sizable field of research, with some dozen Earth satellites now performing measurements or being planned or prepared for launch. Stratospheric measurements are largely those having to do with the photochemistry of the ozone layer, particularly including ozone itself, but also molecules involved in the catalytic cycles which modulate the ozone concentration, including NO_2, BrO, and OClO. Tropospheric measurements of chemical constituents, their sources, sinks, transport, and transformation, provide critical information on tropospheric oxidation chemistry and pollution of the lower atmosphere. Aerosol and cloud measurements in the ultraviolet and visible are not included in this review although they are, of course, also of primary importance.

This review is necessarily too limited by space to be fully inclusive of techniques, groups, and results, and to present a full bibliography. It is rather intended to give the flavor of research in the field, summarize many of the technical issues involved in data analysis, and provide a convenient starting place for further inquiries. The examples presented are primarily taken from research done at the Harvard-Smithsonian Center for Astrophysics (CfA), along with our collaborators, and from a comprehensive survey of colleagues who are currently active in the field to help determine important current issues. After a brief historical background, instrumental approaches and data analysis issues will be discussed and then several of the most timely uses, with current examples, will be presented.

There is not usually a clear distinction between what is properly a spectrometer, making multi-species spectroscopic measurements over a substantial range of wavelength at moderate to high spectral resolution, and an instrument measuring at several wavelength bands to measure (normally) one species. Instruments at both extremes have contributed historically and continue to do so, although there is a marked tendency in the UV/visible to employ spectrometers with array-type detectors to cover large portions of the spectrum at 0.2–1.0 nm spectral resolution. These measurements are emphasized here.

2. Historical background

In a series of papers beginning in 1879, Cornu presented evidence that a terrestrial absorber substantially blocked penetration of solar radiation to the Earth's surface shortward of about 300 nm [1–3]. Hartley demonstrated that this was due to absorption by ozone [4]. The basic techniques were developed early: By the 1890s Langley and Abbot of the Smithsonian Institution had undertaken an extensive program of ground-based measurements of the solar spectrum at the newly-founded Smithsonian Astrophysical Observatory [5]. These measurements employed Langley's recently invented bolometer to make measurements from the infrared through the near ultraviolet in order to determine the mean value of the solar constant and its variation. Langley and Abbot also developed substantial new experimental techniques (such as an early chart recorder) and various analysis techniques (e.g., the 'Langley plot'), including photographic techniques for high and low pass filtering to produce line spectra from 'bolographs' (spectra), illustrated in Fig. 1, foreshadowing the low pass filtering used today by researchers employing the DOAS technique for analyzing atmospheric spectra [6].

Early ground-based measurements continued through the work of Fabry and Buisson [7] who confirmed Cornu and Hartley's demonstration that ozone is located primarily well above the ground level. Systematic spectroscopic measurements of the ozone

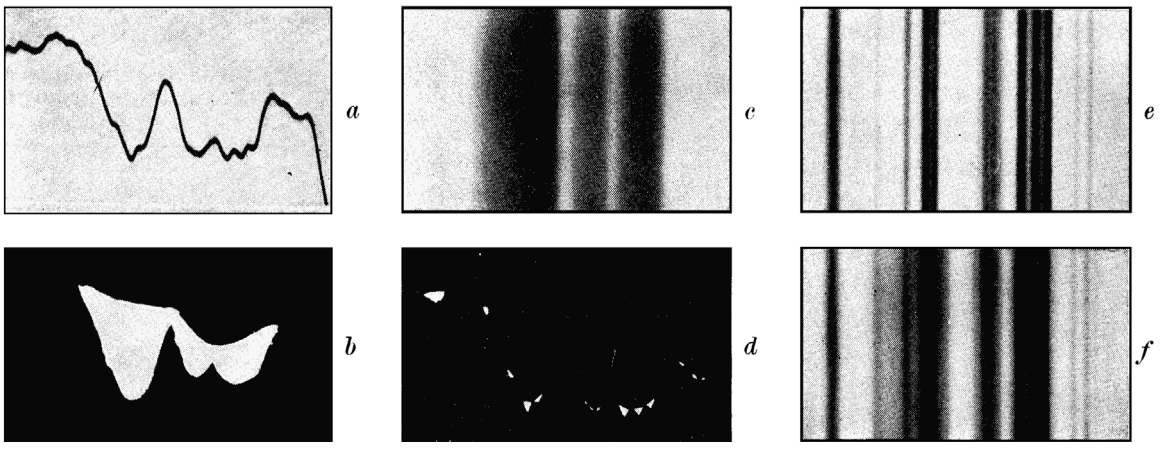

Fig. 1. Photographic production of line spectra from bolographs [5].

layer and its variability began under Dobson in the 1920s [8]. A particularly important example of ground-based measurements are those of NO_2 by Noxon, whose extensive studies determined the existence of the so-called *Noxon cliff*, wherein the HNO_3 sink substantially depletes active nitrogen at higher latitudes in the winter and early spring, contributing to the formation of the ozone hole [9,10].

Ground based spectroscopic measurements in the UV/visible continue to play a fundamental role in atmosphere measurements. These have been supplemented and extended by balloon- and aircraft-based measurements, not presented here, as well as the satellite measurements that are the subject of this article.

3. The UV/visible atmosphere

The solar spectrum can be roughly approximated as a blackbody at 5900 K. The reality, for detailed spectroscopic measurements, is much more complicated. Fig. 2 (upper) shows a low resolution extraterrestrial solar spectrum over much of the UV/visible region [11–13]; Fig. 2 (lower) shows a detailed section of the solar spectrum (the *Fraunhofer* spectrum) in a region where NO_2 is commonly measured from space [11]. The source spectrum is seen to be quite complex. To the extent that measurements correspond to simple *Bouguet* (or *Lambert-Beer*) absorption this would not present a particular difficulty. In practice, because of the *Ring effect* (discussed below in *Technical Challenges*), a detailed knowledge of the solar spectrum is commonly required, particularly for some of the molecules with small absorption: These molecules (including NO_2, BrO, HCHO, OClO, SO_2, and, in parts of the spectrum, O_3) turn out to be often the most important species to be measured from space.

Fig. 3 shows an overview of the absorptions due to molecules that are now commonly measured from space in the nadir geometry. Absorptions are for typical measurement geometry and atmospheric concentrations, except that SO_2 is increased to an amount typical for a volcanic source and OClO is increased to an amount typically seen in the Antarctic polar vortex. The effects of clouds and of Rayleigh scattering can be gauged from Fig. 4, which shows back scattered albedo spectra ($\equiv \pi R/\mu_0 I_0$, where R is the radiance, μ_0 the secant of the solar zenith angle, and I_0 the irradiance) from GOME measurements [14] for two extreme examples. The highest albedo scene, corresponding to full coverage by high clouds, is white and quite bright, due to the cloud reflectance; the lowest albedo case is a cloud-free scene over the ocean illustrating the low reflectance by water (less than 2% at the infrared end) and the increasing contribution from Rayleigh scattering at shorter wavelengths.

4. Techniques

UV/visible measurements of the atmosphere are made in one of three basic measurement geometries:

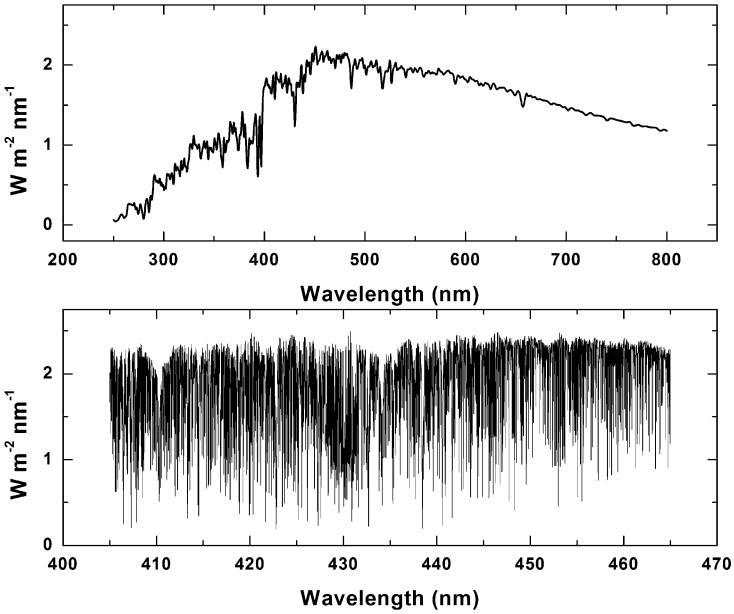

Fig. 2. The low resolution extraterrestrial solar spectrum over much of the UV/visible region (top); a detailed section of the solar spectrum in a region where NO_2 is commonly measured from space (bottom).

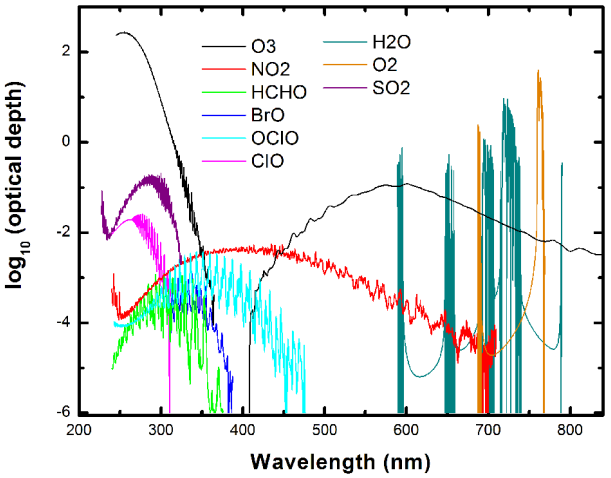

Fig. 3. Typical absorptions due to molecules that are now commonly measured from space in the nadir geometry.

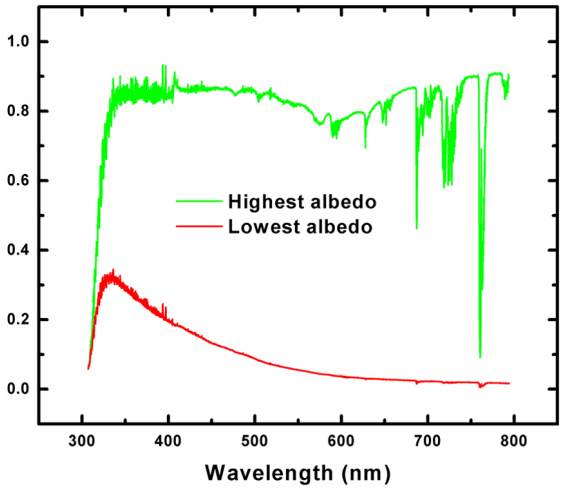

Fig. 4. Back scattered albedo spectra from GOME measurements for two extreme examples. The highest albedo scene, corresponding to full coverage by high clouds, is white and quite bright, due to the cloud reflectance; the lowest albedo case is a cloud-free scene over the ocean.

1. Nadir—the back scattered light is measured in a geometry where the line of sight intersects the Earth's surface. The light source is solar radiation back scattered from a combination of surface reflectance and cloud, aerosol and Rayleigh scattering.
2. Occultation—the light source is direct illumination by the Sun (or, less frequently, the Moon or stars).
3. Limb scattering—the light source is Rayleigh scattering of solar light in the limb geometry. This technique is generally limited to measurements in the stratosphere and upper troposphere.

4.1. Nadir measurements

Analysis of nadir measurements is most commonly made using either fitting to determine a total *slant column* (SC) abundance, followed by adjustment to determine the *vertical column* (VC) abundance, or by directly fitting to details in the spectrum to determine a vertical column amount or profile.

For slant column measurements, spectra may be fitted by a variety of methods, ranging from directly fitting to the radiance, cf. [15] to fitting of a low-pass filtered version of $\ln(R/I_0)$ (i.e., *DOAS*, cf. [6]). Vertical column abundances are then determined by division of the SC by an *Air Mass Factor* (AMF), which is simply the ratio of the slant to vertical column, determined from climatological knowledge of the vertical distribution and radiative transfer calculation to take into account Rayleigh and other scattering as well as the spherical atmospheric geometry (cf. [6,16]). There may be further correction to account for the (sometimes strong) variation of the AMF over the spectral fitting window. It is also possible to fit to vertical column abundances directly, by including the radiative transfer modeling inside of the fitting procedure [17].

It was discovered by Singer and Wentworth [18] that Rayleigh scattering, which often complicates retrieval due to its strong ($\approx 1/\lambda^4$) dependence on wavelength, could also serve as a source of information. In the strong Hartley band of ozone at wavelengths < 300 nm, back scattered radiation has not penetrated to the Earth's surface. The source of illumination is Rayleigh scattering, and light of different wavelengths penetrates to different atmospheric depths, depending on the measurement geometry, the strength of the scattering and the wavelength dependence of the O_3 absorption: The spectrum can be inverted to give a stratospheric ozone profile. This is the basis for BUV/SBUV measurements of ozone profiles [19]. The greater wavelength coverage and higher spectral resolution of more modern spectrometers can improve the situation further. During the sensitivity analyses performed when the SCIAMACHY instrument was being proposed, it was discovered that adding detailed measurements of the strongly temperature-dependent Huggins bands of ozone to the BUV information makes it possible to determine the full atmospheric profile, which includes the tropospheric ozone abundance, directly [20]. This has been the basis of retrievals now successfully made on GOME satellite measurements, discussed below in *Examples*.

4.2. Occultation measurements

Solar occultation measurements from space now have a long and successful heritage. The technique is deceptively simple, requiring pointing to the Sun and inversion of sets of slant column measurements using ephemeris data and correcting for atmospheric refraction. The reality is more complex: The SAGE instruments, for example, raster vertically over the Sun in order to be able to take into account variations of intensity over the solar disk as well as distortion of the solar image by refraction at lower altitudes [21]. Stellar occultation is now used by the GOMOS instrument to extend the ability to measure NO_2 and O_3 globally, to avoid the limitations in geographic coverage inherent in solar occultation measurements from space (http://envisat.esa.int/instruments/gomos). Lunar occultation measurements are rarer, but are now performed by SCIAMACHY, with the intention of extending the coverage to (limited) nighttime measurements [20,22].

4.3. Limb scattering measurements

Analysis of limb scattered light is more complex than analysis of occultations. First, the light source (principally Rayleigh scattering) is more diffuse and requires careful modeling of the Rayleigh source function and its variation along the measurement path. Detailed knowledge of the instrument field-of-view, and of multiple scattering from lower atmospheric layers, particularly over bright scenes, are required. These complications make inversion of slant column abundances to vertical concentration profiles particularly challenging. Second, the limb pointing cannot necessarily be reliably determined from spacecraft pointing and ephemeris data but must, in the general case, be determinable from the data themselves. Fortunately, for instruments which include the Hartley-Huggins ozone spectral range, there is a 'knee' in the brightness versus tangent altitude, caused by competition between increased scattering and increase O_3 absorption, that may be used to determine the pointing to several hundred meters under favorable circumstances [23,24].

5. Technical challenges

This section summarizes a number of the technical challenges that have had to be addressed in order to successfully analyze UV/visible atmospheric spectra from satellites to the fine level of agreement (as low as several times 10^{-4} of measured radiances in favorable cases) needed for use in atmospheric process studies.

5.1. Detectors

The current generation of satellite spectrometers (summarized below in *Instruments*) utilize either 1-dimensional silicon diode array detectors (usually Reticon® detectors) or 2-dimensional CCD devices. Of the two choices, the diode array detectors offer the best performance on a per-pixel basis, having large well depths and generally lower dark current. In the most favorable cases, it has been possible to fit GOME spectra, for example, to an RMS of $< 3 \times 10^{-4}$ of the full scale radiance [15]. CCD detectors at present achieve lower performance on a per-pixel basis but enable multiple spectra to be obtained simultaneously, i.e., spectrum in one dimension and across-track ground pixel position in the other. Future instruments will likely benefit from the use of 2-D silicon diode array technology which has recently become available in sufficiently large formats, and combines the advantages of both previous types.

5.2. Solar reference spectra

An extraterrestrial high resolution solar spectrum would be invaluable for the spaceborne measurements. Such a spectrum is needed for wavelength calibration [25], Ring effect determination [26–28], determination of the instrument transfer function from flight data, and correction for spectral undersampling [29]. Since an appropriate extraterrestrial spectrum does not exist (the extensive SOLSTICE/SUSIM measurements of [12] are very good in absolute intensity calibration, but have much too low spectral resolution to be used for these purposes), ground-based FTS spectra, in particular a solar spectrum from Kurucz et al. at the National Solar Observatory (NSO) [11] has been used extensively, supplemented at wavelengths <305 nm by balloon-based spectra from Hall and Anderson [30].

5.3. Rayleigh scattering and the Ring effect

Rayleigh scattering is a major contributor, sometimes the predominant contributor, to back scattered light measured in the nadir, depending on wavelength and detailed measurement geometry. For limb measurements, it is the source of the measured

light, except for aerosol contributions at lower altitudes. Highly accurate formulations of the wavelength dependences of the cross sections and scattering phase function for Rayleigh scattering by air are available [26,31,32].

The Ring effect was first noted by Grainger and Ring [33] as a broadening and reduction in depth of solar Fraunhofer lines when viewed from the ground in scattered sunlight. It has now been firmly demonstrated to be the effect of the fraction of Rayleigh scattering by air that is inelastic, i.e., Raman scattering. The Raman scattering is predominantly rotational Raman; it constitutes 4% of the Rayleigh scattering in the UV/visible. Ring effect corrections may be performed using the molecular physics of the Raman scattering coupled with a suitable solar reference spectrum [27], in some cases coupled with radiative transfer calculations [26,28], to the level that negligible uncertainties remain in the spectral fitting from this source of spectral structure.

Vibrational Raman scattering in ocean water can be readily sensed in the UV/visible (it must be corrected for in the spectral analysis for some gases) and it has been suggested that it may be used to "*estimate chlorophyll and dissolved organic matter contents*" of ocean water [34].

5.4. Wavelength issues

Ground-based wavelength calibration is insufficient for detailed spectrum fitting of satellite data for several reasons. First, calibration can shift substantially due to launch stresses; second, calibration in flight can vary by substantial amounts, compared to the spectral fitting needs, due to thermal and other in-flight perturbations and instrumental effects (e.g., partial filling of the field-of-view); third, solar irradiances and radiances are often obtained (especially for nadir observations) at substantially different Doppler shifts (up to 0.01 nm at 400 nm). For these reasons, methods were developed first for GOME in-flight spectral calibration, using nonlinear least-squares (NLLS) minimization or spectral cross correlation, where the comparison spectrum in both cases is derived from the NSO spectrum described above [25]. The NLLS method is now used extensively in scientific analyses, and has been implemented in operational algorithms for GOME, SCIAMACHY, OMI, and OMPS.

5.5. Reference spectra

Reference spectra for UV/visible measurements are now included in the HITRAN database [35,36], and regularly updated. Reference spectra are published sometimes with vacuum wavelengths and sometimes with air wavelengths (often with insufficient detail of laboratory conditions to allow accurate conversion to vacuum). It is highly recommended that vacuum wavelengths be the standard, and that accurate conversion be made when necessary. Highly accurate conversion formulae are available [32]. As UV/visible reference spectra are increasingly determined using Fourier transform spectrometers, this becomes less of an issue, since wavenumbers (cm^{-1}) are intrinsically in vacuum.

5.6. Instrument function and sampling issues

Slit functions (instrument transfer functions, ITFs) in flight may differ from those determined in ground calibration. It is often useful to re-determine them in flight. The normal procedure is to combine this fitting with the wavelength calibration using NLLS, where the reference spectrum is a high-resolution solar spectrum. Spectral undersampling occurs in array-based instruments (or indeed any spectrometer) when spectral measurements are not made at fine enough spacing to *Nyquist sample* the ITF [37], and thus provide full knowledge of the spectrum up to the band limit (Nyquist sampling requires sampling to at least twice the highest spatial (i.e., wavelength) frequency admitted by the resolution limit of the instrument). It can be a major source of fitting error in the current generation of satellite-borne spectrometers, particularly as solar irradiance spectra must be resampled in order to be compared to radiances in the spectral fitting process [15]. Where the trace gas absorptions are optically thin, it is possible to effectively correct for most of the undersampling error [15,38]. It is now possible to quantitatively determine the amount a spectrum will be undersampled (or, how close it is to being fully-sampled) for a given instrument configuration during the design phase [29].

5.7. Radiative transfer modeling and chemistry and transport modeling

Radiative transfer calculations, usually requiring multiple scattering treatment, and often needing spherical correction or inclusion of polarization, are fundamental to the analysis of UV/visible measurements in nadir and limb geometries. Radiative transfer models are now available for most UV/visible measurement situations [39–46].

Primarily because of the interference by Rayleigh scattering with geometrical scattering paths in nadir measurements, particularly for tropospheric measurements, it is often necessary to couple radiative transfer calculations with chemistry and transport modeling in order to determine AMFs: The contribution of molecular absorption to back scattered radiance depends significantly on the absorber altitude. Generally, absorbers at lower altitudes contribute less to the observed signal (cf. [16]). The GEOS-CHEM and MOZART 3-D tropospheric chemistry and transport models [47–49] are in common use for this purpose.

6. Instruments

A series of satellite instruments which measured in discrete (sometimes scannable) spectral bands formed the foundation for present satellite spectrometers. The BUV/SBUV instruments, 1970-present (cf. [50]) and the TOMS instruments, 1978-present (cf. [51]) are predecessors of current spectroscopic UV/visible nadir instruments. The SAGE I and II instruments [21] and the Solar Mesosphere Explorer [52] are predecessors for current occultation instruments. Current and planned instruments are summarized in Table 1.

Table 1
Current and planned UV/visible satellite spectrometers

Instrument/Platform	Wavelength range (nm)	Viewing geometry	Primary gases	Launch year
GOME/ERS-2; GOME-2/MetOp (×3)	240–790	Nadir	O_3, NO_2, BrO, OClO, SO_2, HCHO, H_2O	1995+
OSIRIS/Odin	280–800	Limb	O_3, NO_2, BrO, OClO, SO_2, HCHO	2001
SAGE III/Meteor-3M (2 additional planned)	280–1040	Occultation (limb)	O_3, NO_2, NO_3, BrO, OClO, H_2O	2001
GOMOS/Envisat	250–952	Stellar occultation	O_3, NO_2, NO_3, H_2O	2002
SCIAMACHY/Envisat	240–2340	Nadir/limb/ occultation	O_3, NO_2, BrO, OClO, SO_2, HCHO, H_2O, NO_3 (plus infrared gases)	2002
MAESTRO/ACE	285–1030	Occultation	O_3, NO_2, BrO, OClO, SO_2, HCHO, H_2O	2003
OMI/EOS-Aura	270–500	Nadir	O_3, NO_2, BrO, OClO, SO_2, HCHO	2004
OPUS/GCOM	306–420	Nadir	O_3, NO_2, BrO, OClO, SO_2, HCHO	2007
OMPS/NPP-NPOESS (×4)	259–1000	Nadir/limb	O_3, NO_2, BrO, OClO, SO_2, HCHO, H_2O	2008+

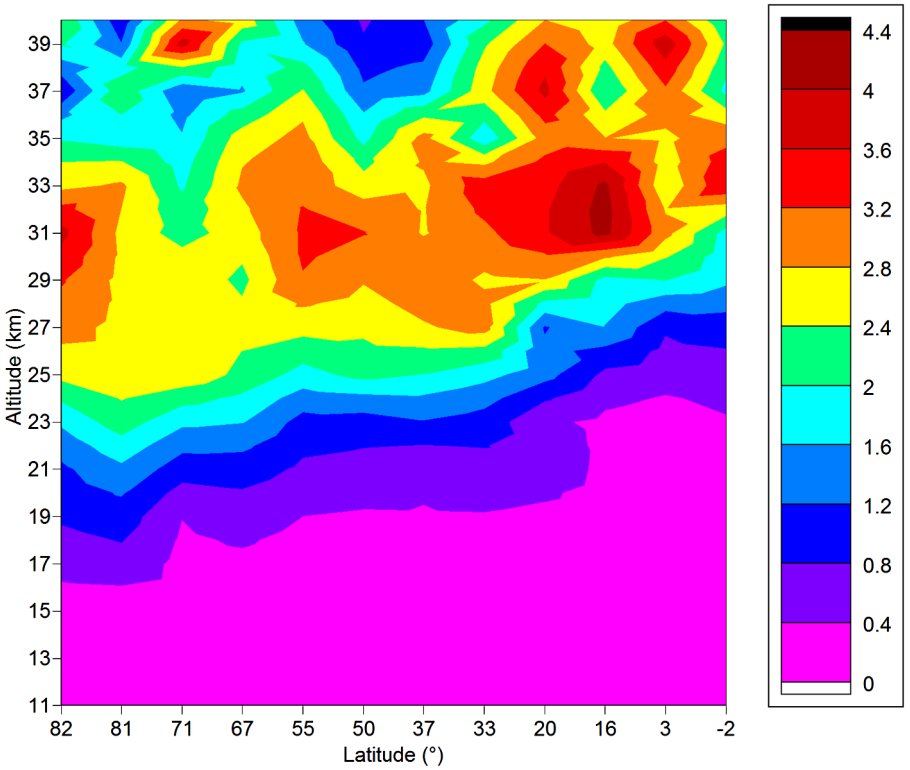

Fig. 5. Meridional cross-section of the NO_2 volume mixing ratio (ppbv) from an orbit of OSIRIS on the morning of April 8, 2004 [24]. Excess NO_2 from earlier solar storms descends into the upper stratosphere at high northern latitudes.

7. Scientific examples

7.1. Stratospheric and tropospheric NO_2

Stratospheric NO_2 is measured globally by several instruments, using occultations, limb scattering and nadir measurements. Fig. 5 shows the meridional cross-section of the NO_2 volume mixing ratio (ppbv) from an orbit of OSIRIS on the morning of 8 April 2004 [24] (courtesy of C.E. Sioris). Excess NO_2 from earlier solar storms descends into the upper stratosphere at high northern latitudes. The GOMOS instrument employs stellar occultation to obtain global maps of NO_2 and several other molecules throughout the diurnal cycle. Fig. 6 shows latitude-altitude maps of nighttime NO_2 mixing ratios for the months October–December 2003. The strong maximum in the upper stratosphere at high north latitudes is due to the strong production of NO_x during the 28 October solar proton event (courtesy of A. Hauchecorne and J.-L. Bertaux).

Nitrogen dioxide is the primary measurable proxy for NO_x, the reactive nitrogen pollutants. Satellite measurements are used to track pollution and to improve global NO_x emission inventories [53], and for other detailed process studies, such as the release of NO_x from soils [54]. Fig. 7 shows global tropospheric NO_2 derived from SCIAMACHY measurements for May-October 2004, during the 2004 International Consortium for Atmospheric Research on Transport and Transformation (ICARTT) campaign (courtesy of R.V. Martin and C.E. Sioris).

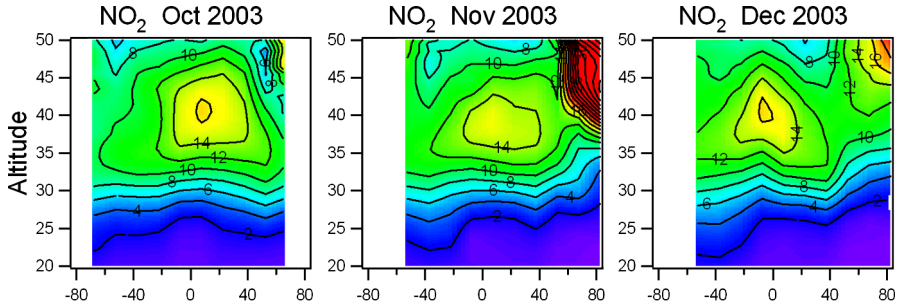

Fig. 6. Latitude-altitude maps of nighttime NO_2 mixing ratios for the months Oct.–Dec. 2003 The strong maximum in upper stratosphere at high north latitudes is due to the strong production of NO_x during the 28 October solar proton event.

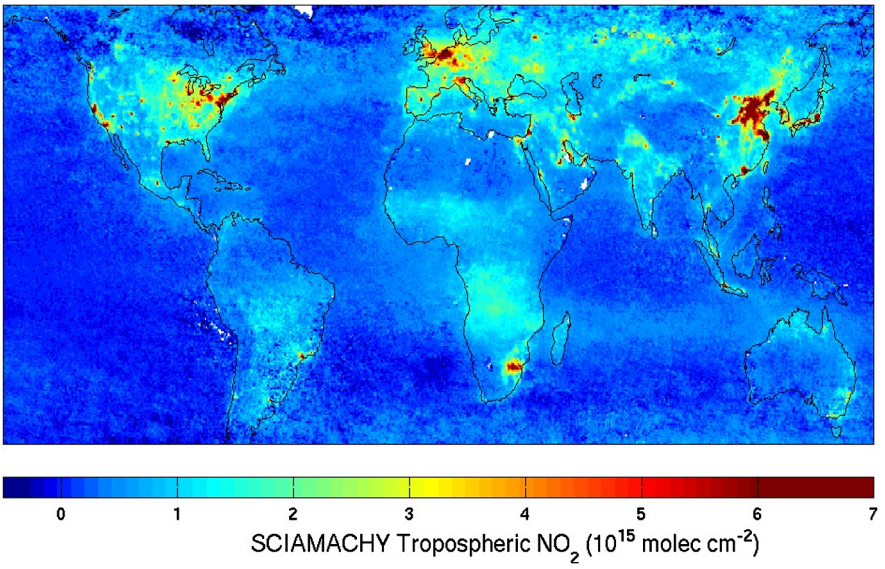

Fig. 7. Tropospheric NO_2 from SCIAMACHY during the 2004 ICARTT campaign. Pollution on urban scales is readily measured globally.

7.2. BrO in polar spring conditions

Initial sensitivity studies for GOME and SCIAMACHY indicated that stratospheric BrO would be measurable globally [20]. It was later discovered, from ground-based measurements [55] and then confirmed by GOME measurements that BrO is released copiously from the ice pack in polar spring, in both hemispheres. Fig. 8 shows northern hemisphere BrO derived from GOME measurements for 30 April – 2 May 1997, illustrating the large enhancements over the ice pack.

7.3. Global HCHO measurements

Formaldehyde is the primary measurable proxy for volatile organic compounds, VOCs. Tropospheric HCHO measurements derived from GOME are used to improve VOC emission inventories [56]. Fig. 9 shows our tropospheric formaldehyde (HCHO) measurements from GOME for July 1996. High HCHO regions reflect VOC emissions from fires, the biosphere (e.g., isoprene emissions from stressed vegetation), and human activity (courtesy of P.I. Palmer).

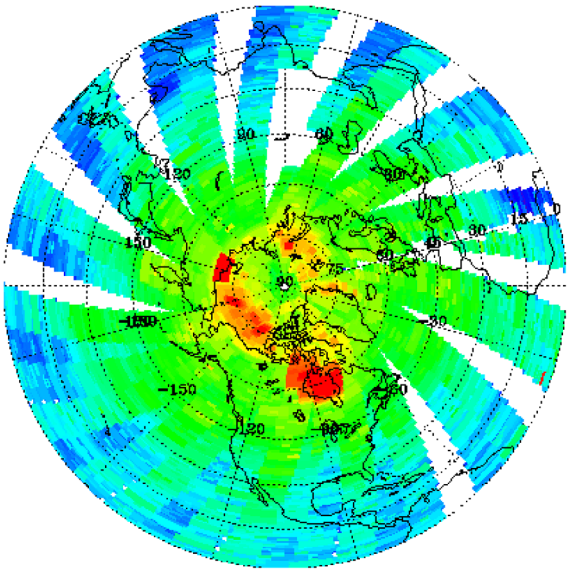

Fig. 8. Northern hemisphere BrO derived from GOME measurements for 30 April – 2 May 1997, illustrating the large enhancements over the ice pack.

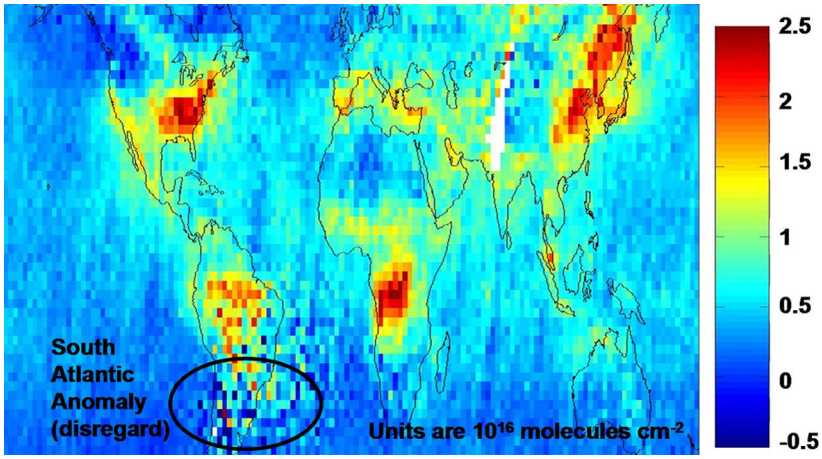

Fig. 9. Tropospheric formaldehyde (HCHO) measurements from GOME for July 1996. High HCHO regions reflect VOC emissions from fires, the biosphere and human activity.

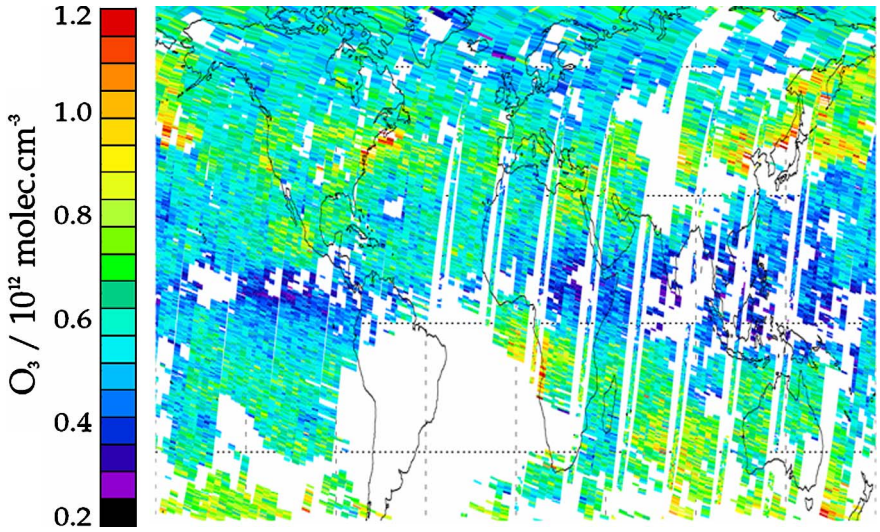

Fig. 10. Surface level ozone density derived by the Rutherford Appleton Laboratory from 25–27 June, 2000 GOME measurements.

7.4. Tropospheric ozone

Initial sensitivity studies for GOME and SCIAMACHY indicated that tropospheric ozone would be measurable globally [20]. This was first demonstrated with GOME flight data by the Rutherford Appleton Laboratory [57], and has since been implemented by several other groups, including the CfA. Fig. 10 shows the surface level ozone density derived from 25–27 June 2000 GOME measurements (courtesy of R. Siddans).

8. Conclusions

Spaceborne remote sensing of the Earth's atmosphere utilizing ultraviolet and visible spectroscopy is a field that is rapidly reaching maturity. Measurement techniques, instrumentation, and data analysis algorithms have been developed to the point that most of the potential applications have now been solidly demonstrated. Stratospheric measurements determine the details of the photochemistry of the ozone layer, including ozone itself, and several primary gases involved in ozone photochemistry: NO_2, BrO, and (in the polar vortex) OClO. Measurements of the tropospheric pollutants O_3, NO_2, and HCHO quantify important aspects of oxidation chemistry and pollution transport, and are now being used to improve global emission inventories of NO_x and VOCs.

Measurements from satellite instruments now planned will continue for at least the next 20 years, and should form the basis for improved environmental monitoring systems to monitor atmospheric pollution globally and continuously from space. Employing capabilities that have now been demonstrated from geostationary orbit is an obvious approach to accomplishing this goal.

Acknowledgements

I owe particular thanks to my collaborators and colleagues for generously sharing their figures for inclusion here: Randall V. Martin, Christopher E. Sioris, Paul I. Palmer, Richard Siddans, Brian J. Kerridge, Alain Hauchecorne, and Jean-Loup Bertaux. The preparation of this review was supported by the Smithsonian Institution. Research at the CfA has been supported by NASA and the Smithsonian Institution. The cooperation of the European Space Agency and the German Aerospace Center is, as always, greatly appreciated.

References

[1] A. Cornu, Sur la limite ultra-violette du spectre solaire, C. R. Acad. Sci. Paris 8 (1879) 1101–1108.
[2] A. Cornu, Sur l'absorption par l'atmosphère des radiations ultra-violettes, C. R. Acad. Sci. Paris 88 (1879) 1285–1290.

[3] A. Cornu, Sur la limite ultra-violette du spectre solaire, d'après des clichés obtenus par M. le Dr O. Simony au sommet du pic de Ténériffe, C. R. Acad. Sci. Paris 111 (1890) 941–947.
[4] W.N. Hartley, On the absorption of solar rays by atmospheric ozone, J. Chem. Soc. 39 (1881) 111–128.
[5] S.P. Langley, Abbot C.G., Annals of the Astrophysical Observatory of the Smithsonian Institution 1 (1900) 69–75.
[6] U. Platt, Differential optical absorption spectroscopy (DOAS), in: M.W. Sigrist (Ed.), Air Monitoring by Spectroscopic Techniques, in: Chem. Anal. Ser., vol. 127, John Wiley, New York, 1994, pp. 27–84.
[7] C. Fabry, Buisson H., L'absorption de l'ultraviolet par l'ozone et la limite du spectre solaire, J. Phys. Paris 3 (1913) 196–206.
[8] G.M.B. Dobson, Forty years' research on atmospheric ozone at Oxford: A history, Appl. Opt. 7 (1968) 387–405.
[9] J.F. Noxon, Stratospheric NO_2 in the Antarctic winter, Geophys. Res. Lett. 5 (1978) 1021–1022.
[10] J.F. Noxon, Stratospheric NO_2, 2, Global behavior, J. Geophys. Res. 84 (1979) 5067–5076.
[11] R.L. Kurucz, I. Furenlid, J. Brault, L. Testerman, Solar Flux Atlas from 296 to 1300 nm, National Solar Observatory, Sunspot, New Mexico, 1984, 240 pp.
[12] T.N. Woods, D.K. Prinz, G.J. Rottman, J. London, P.C. Crane, R.P. Cebula, E. Hilsenrath, G.E. Brueckner, M.D. Andrews, O.R. White, M.E. VanHoosier, L.E. Floyd, L.C. Herring, B.G. Knapp, C.K. Pankratz, P.A. Reiser, Validation of the UARS solar ultraviolet irradiances: Comparison with the ATLAS 1 and 2 measurements, J. Geophys. Res. 101 (1996) 9541–9570.
[13] A. Berk, G.P. Anderson, L.S. Bernstein, P.K. Acharya, H. Dothe, M.W. Matthew, S.M. Adler-Golden, J.H. Chetwynd Jr., S.C. Richtsmeier, B. Pukall, C.L. Allred, L.S. Jeong, M.L. Hoke, MODTRAN4 radiative transfer modeling for atmospheric correction, Proc. SPIE, Optical Spectroscopic Techniques and Instrumentation for Atmospheric and Space Research III 3756 (1999) 348–353.
[14] GOME Users Manual, ESA Special Publication SP-1182, ESTEC, Noordwijk, 1995.
[15] K. Chance, Analysis of BrO measurements from the Global Ozone Monitoring Experiment, Geophys. Res. Lett. 25 (1988) 3335–3338.
[16] P.I. Palmer, D.J. Jacob, K. Chance, R.V. Martin, R.J.D. Spurr, T.P. Kurosu, I. Bey, R. Yantosca, A. Fiore, Q. Li, Air mass factor formulation for spectroscopic measurements from satellites: Application to formaldehyde retrievals from the Global Ozone Monitoring Experiment, J. Geophys. Res. 106 (2001) 14539–14550.
[17] R. Spurr, M. van Roozendael, J. Lambert, C. Fayt, The GODFIT direct fitting algorithm: A new approach for total column retrieval, in: Proc. 2004 ENVISAT & ERS Symposium, ESA publication SP-572, 2004.
[18] S.F. Singer, R.C. Wentworth, A method for the determination of the vertical ozone distribution from a satellite, J. Geophys. Res. 62 (1957) 299–308.
[19] D.F. Heath, C.L. Mateer, A.J. Krueger, The Nimbus-4 backscatter ultraviolet (BUV) atmospheric ozone experiment—two years' operation, Pure Appl. Geophys. 106–108 (1973) 1238–1253.
[20] K.V. Chance, J.P. Burrows, W. Schneider, Retrieval and molecule sensitivity studies for the Global Ozone Monitoring Experiment and the SCanning Imaging Absorption spectroMeter for Atmospheric CHartographY, Proc. S.P.I.E., Remote Sensing of Atmospheric Chemistry 1491 (1991) 151–165.
[21] L.E. Mauldin III, N.H. Zaun, M.P. McCormick Jr., J.H. Guy, W.R. Vaughn, Stratospheric aerosol and gas experiment II instrument: A functional description, Opt. Eng. 24 (1985) 307–312.
[22] S. Noël, J.P. Burrows, H. Bovensmann, J. Frerick, K.V. Chance, A.P.H. Goede, C. Muller, Atmospheric trace gas sounding with SCIAMACHY, Adv. Space Res. 26 (2000) 1949–1954.
[23] R.D. McPeters, S.J. Janz, E. Hilsenrath, T.L. Brown, The retrieval of O_3 profiles from limb scatter measurements: Results from the Shuttle Ozone Limb Sounding Experiment, Geophys. Res. Lett. 27 (2000) 2597–2600.
[24] C.E. Sioris, C.S. Haley, C.A. McLinden, C. von Savigny, I.C. McDade, W.F.J. Evans, J.C. McConnell, N.D. Lloyd, E.J. Llewellyn, D. Murtagh, U. Frisk, T.P. Kurosu, K.V. Chance, K. Pfeilsticker, H. Bösch, F. Weidner, Stratospheric profiles of nitrogen dioxide observed by optical spectrograph and infrared imager system on the Odin satellite, J. Geophys. Res. 108 (2003) 4215, doi:10.1029/2002JD002672.
[25] C. Caspar, K. Chance, GOME wavelength calibration using solar and atmospheric spectra, in: T.-D. Guyenne, D. Danesy (Eds.), Proc. Third ERS Symposium on Space at the Service of our Environment, European Space Agency Special Publication SP-414, 1997.
[26] J. Joiner, P.K. Bhartia, R.P. Cebula, E. Hilsenrath, R.D. McPeters, H. Park, Rotational Raman scattering (ring effect) in satellite backscatter ultraviolet measurements, Appl. Opt. 34 (1995) 4513–4525.
[27] K. Chance, R.J.D. Spurr, Ring effect studies: Rayleigh scattering, including molecular parameters for rotational Raman scattering, and the Fraunhofer spectrum, Appl. Opt. 36 (1997) 5224–5230.
[28] M. Vountas, V.V. Rozanov, J.P. Burrows, Ring effect: Impact of rotational Raman scattering on radiative transfer in Earth's Atmosphere, J. Quant. Spectrosc. Radiat. Transfer 60 (1998) 943–961.
[29] K. Chance, T.P. Kurosu, C.E. Sioris, Undersampling correction for array detector-based satellite spectrometers, Appl. Opt. 44 (2005) 1296–1304.
[30] L.A. Hall, G.P. Anderson, High-resolution solar spectrum between 200 and 3100 Å, J. Geophys. Res. 96 (1991) 12927–12931.
[31] D.R. Bates, Rayleigh scattering by air, Planet. Space Sci. 32 (1984) 785–790.
[32] B.A. Bodhaine, N.B. Wood, E.G. Dutton, J.R. Slusser, On Rayleigh optical depth calculations, J. Atmos. Ocean. Tech. 16 (1999) 1854–1861.
[33] J.F. Grainger, J. Ring, Anomalous Fraunhofer line profiles, Nature 193 (1962) 762.
[34] A.P. Vasilkov, J. Joiner, J. Gleason, P.K. Bhartia, Ocean Raman scattering in satellite backscatter UV measurements, Geophys. Res. Lett. 29 (2002) 1837, doi:10.1029/2002GL014955.
[35] L.S. Rothman, A. Barbe, D.C. Benner, L.R. Brown, C. Camy-Peyret, M.R. Carleer, K. Chance, C. Clerbaux, V. Dana, V.M. Devi, A. Fayt, J.-M. Flaud, R.R. Gamache, A. Goldman, D. Jacquemart, K.W. Jucks, W.J. Lafferty, J.-Y. Mandin, S.T. Massie, V. Nemtchinov, D.A. Newnham, A. Perrin, C.P. Rinsland, J. Schroeder, K.M. Smith, M.A.H. Smith, K. Tang, R.A. Toth, J. Vander Auwera, P. Varanasi,

K. Yoshino, The HITRAN molecular spectroscopic database: Edition of 2000 including updates through 2001, J. Quant. Spectrosc. Radiat. Transfer 82 (2003) 5–44.
[36] J. Orphal, K. Chance, Ultraviolet and visible absorption cross sections for HITRAN, J. Quant. Spectrosc. Radiat. Transfer 82 (2003) 491–504.
[37] S. Goldman, Information Theory, Prentice-Hall, New York, 1953.
[38] S. Slijkhuis, A. von Bargen, W. Thomas, K. Chance, Calculation of undersampling correction spectra for DOAS spectral fitting, in: Proc. ESAMS'99—European Symposium on Atmospheric Measurements from Space, 1999, pp. 563–569.
[39] R.J.D. Spurr, T.P. Kurosu, K. Chance, A linearized discrete ordinate radiative transfer model for atmospheric remote sensing retrieval, J. Quant. Spectrosc. Radiat. Transfer 68 (2001) 689–735.
[40] R.J.D. Spurr, LIDORT V2PLUS: A comprehensive radiative transfer package for UV/VIS/NIR nadir remote sensing; A general quasi analytic solution, in: Proc. S.P.I.E., vol. 5235, Remote Sensing of Clouds and the Atmosphere VIII, 2003.
[41] R.F. Van Oss, R.J.D. Spurr, Fast and accurate 4-stream linearized discrete ordinate radiative transfer models for ozone profile retrieval, J. Quant. Spectrosc. Radiat. Transfer 75 (2002) 177–220.
[42] V.V. Rozanov, D. Diebel, R.J.D. Spurr, J.P. Burrows, GOMETRAN: A radiative transfer model for the satellite project GOME—the plane-parallel version, J. Geophys. Res. 102 (1997) 16683–16695.
[43] V.V. Rozanov, M. Buchwitz, K.-U. Eichmann, R. de Beek, J.P. Burrows, SCIATRAN—a new radiative transfer model for geophysical applications in the 240–2400 nm spectral region: The pseudo-spherical version, Adv. Space Res. 29 (2002) 1831–1835.
[44] C.A. McLinden, J.C. McConnell, E. Griffioen, C.T. McElroy, A vector radiative transfer model for the Odin/OSIRIS project, Can. J. Phys. 80 (2002) 375–393.
[45] J.F. De Haan, P.B. Bosma, J.W. Hovenier, The adding method for multiple scattering calculations of polarized light, Astron. Astrophys. 183 (1987) 371–391.
[46] P. Stammes, Spectral radiance modelling in the UV-visible range, in: W.L. Smith, Y.M. Timofeyev (Eds.), IRS 2000: Current Problems in Atmospheric Radiation, A. Deepak, Hampton, VA, 2001, pp. 385–388.
[47] I. Bey, D.J. Jacob, R.M. Yantosca, J.A. Logan, B.D. Field, A.M. Fiore, Q. Li, H.Y. Liu, L.J. Mickley, M.G. Schultz, Global modeling of tropospheric chemistry with assimilated meteorology: Model description and evaluation, J. Geophys. Res. 106 (2001) 23073–23096.
[48] G.P. Brasseur, D.A. Hauglustaine, S. Walters, P.J. Rasch, J.-F. Muller, C. Granier, X.X. Tie, MOZART: A global chemical transport model for ozone and related chemical tracers, part 1. Model description, J. Geophys. Res. 103 (1998) 28265–28289.
[49] D.A. Hauglustaine, G.P. Brasseur, S. Walters, P.J. Rasch, J.-F. Muller, L.K. Emmons, M.A. Carroll, MOZART: A global chemical transport model for ozone and related chemical tracers, part 2. Model results and evaluation, J. Geophys. Res. 103 (1998) 28291–28335.
[50] R.D. McPeters, A.J. Krueger, P.K. Bhartia, J.R. Herman, Earth Probe Total Ozone Mapping Spectrometer (TOMS) Data Products User's Guide, NASA Reference Publication 1998-206895, National Aeronautics and Space Administration, Washington, DC, 1998.
[51] A.J. Fleig, R.D. McPeters, P.K. Bhartia, B.M. Schlesinger, R.P. Cebula, K.F. Klenk, S.L. Taylor, D.F. Heath, Nimbus-7 Solar Backscatter Ultraviolet (SBUV) Ozone Products User's Guide, NASA Reference Publication, 1234, National Aeronautics and Space Administration, Washington, DC, 1990.
[52] D.W. Rusch, G.H. Mount, C.A. Barth, R.J. Thomas, M.T. Callan, Solar Mesosphere Explorer Ultraviolet Spectrometer: Measurements of ozone in the 1.0–0.1 mbar region, J. Geophys. Res. 89 (1984) 11677–11687.
[53] R.V. Martin, D.J. Jacob, K. Chance, T. Kurosu, P.I. Palmer, M.J. Evans, Global inventory of nitrogen oxide emissions constrained by space-based observations of NO_2 columns, J. Geophys. Res. 108 (2003) 4537, doi:10.1029/2003JD003453.
[54] L. Jaeglé, R.V. Martin, K. Chance, L. Steinberger, T.P. Kurosu, D.J. Jacob, A.I. Modi, V. Yoboué, L. Sigha-Nkamdjou, C. Galy-Lacaux, Satellite mapping of rain-induced nitric oxide emissions from soils, J. Geophys. Res. 109 (2004) D21310, doi:10.1029/2004JD004787.
[55] K. Kreher, P.V. Johnston, S.W. Wood, B. Nardi, U. Platt, Ground-based measurements of tropospheric and stratospheric BrO at Arrival Heights, Antarctica, Geophys. Res. Lett. 24 (1997) 3021–3024.
[56] P.I. Palmer, D.J. Jacob, A.M. Fiore, R.V. Martin, K. Chance, T. Kurosu, Mapping isoprene emissions over North America using formaldehyde column observations from space, J. Geophys. Res. 108 (2003) 4180, doi:10.1029/2002JD002153.
[57] R. Munro, R. Siddans, W.J. Reburn, B.J. Kerridge, Direct measurement of tropospheric ozone distributions from space, Nature 392 (1998) 168–171.